arXiv:1605.02295v3 [cond-mat.dis-nn] 29 Jun 2016

Non-ergodic phases in strongly disordered random regular graphs.

B. L. Altshuler,[1] E. Cuevas,[2] L. B. Ioffe,[3,4] and V. E. Kravtsov[5,4]

[1]*Physics Department, Columbia University, 538 West 120th Street, New York, New York 10027, USA*
[2]*Departamento de Física, Universidad de Murcia, E30071 Murcia, Spain*
[3]*CNRS and Universite Paris Sud, UMR 8626, LPTMS, Orsay Cedex, F-91405, France*
[4]*L. D. Landau Institute for Theoretical Physics, Chernogolovka, Russia*
[5]*Abdus Salam International Center for Theoretical Physics, Strada Costiera 11, 34151 Trieste, Italy*

We combine numerical diagonalization with a semi-analytical calculations to prove the existence of the intermediate non-ergodic but delocalized phase in the Anderson model on disordered hierarchical lattices. We suggest a new generalized population dynamics that is able to detect the violation of ergodicity of the delocalized states within the Abou-Chakra, Anderson and Thouless recursive scheme. This result is supplemented by statistics of random wave functions extracted from exact diagonalization of the Anderson model on ensemble of disordered Random Regular Graphs (RRG) of N sites with the connectivity $K = 2$. By extrapolation of the results of both approaches to $N \to \infty$ we obtain the fractal dimensions $D_1(W)$ and $D_2(W)$ as well as the population dynamic exponent $D(W)$ with the accuracy sufficient to claim that they are non-trivial in the broad interval of disorder strength $W_E < W < W_c$. The thorough analysis of the exact diagonalization results for RRG with $N > 10^5$ reveals a singularity in $D_{1,2}(W)$-dependencies which provides a clear evidence for the first order transition between the two delocalized phases on RRG at $W_E \approx 10.0$. We discuss the implications of these results for quantum and classical non-integrable and many-body systems.

Introduction.–The concept of Many Body localization (MBL) [1] emerged as an attempt to extend the celebrated ideas of Anderson localization (AL) [2] from one-particle eigenstates formed by a static random potential to the many-body eigenfunctions of macroscopic quantum systems. In Ref.[1] it was analytically demonstrated that cooling of an isolated system of interacting fermions (electrons) with localized one-particle states leads to a metal - insulator finite-temperature transition which can be described as MBL in the Fock space. Later on the MBL in various models (XXZ spin chain subject to a random magnetic field [3, 4], array of Josephson junctions [5], etc.) became a subject of intensive theoretical studies.

The ideas of MBL appear naturally in discussions of applicability of the conventional Boltzmann-Gibbs statistical mechanics to isolated many-body systems. This description based on the equipartition postulate should not be valid for the localized many-body states. Moreover, in Ref. [5] it was shown that Boltzmann-Gibbs description of the isolated Josephson arrays most likely remains invalid even in so called "bad metal" phase where the eigenstates are extended but not ergodic, e.g. they occupy a vanishing fraction of the Hilbert space.

There are reasons to believe [6] that properties of a one-particle Anderson model (tight-binding model with on-site disorder) on hierarchical lattices such as the Bethe lattice (BL) strongly resemble generic properties of a wide class of many-body models. BL is characterized by (i) the exponential dependence of the number of sites $N = K^R$ (which is analogous to the dimension of the Hilbert space in MBL) on the radius of the tree R with the branching number K and (ii) the absence of loops. The latter simplifies the problem of AL as compared to AL in finite dimensions. In the seminal paper [7] Abou-Chakra, Anderson and Thouless developed an analytical approach to the Anderson model on an infinite BL that allowed them not only to demonstrate the existence of the AL transition but also to evaluate the critical disorder with a pretty good accuracy. More recently some mathematically rigorous results, e.g. the proof of the existence of extended states and the refined position of the mobility edges were obtained [8, 9].

Nonetheless, the most interesting and the least studied aspect of AL on the BL is the statistics of extended wave functions. Recently it has been suggested in Refs.[10, 11] (see also [18]) that these statistics may be multifractal, i.e. extended states in a broad interval of disorder strength may be non-ergodic. The contradiction of this statement with the earlier studies [12] provoked a vigorous discussion [13–17].

Note that the mere formulation of statistics of normalized extended wave functions in a *closed* system requires understanding of the thermodynamic limit of a *finite-size* problem. For BL this poses a major problem: a finite fraction of sites belongs to the boundary making the results crucially dependent on the boundary conditions. A known remedy [10, 11] is to consider a Random Regular Graph (RRG)[19, 20], thus realizing the boundary-less hierarchical system which is locally tree-like.

In this paper we reformulate the approach of Ref.[7] in a way that distinguishes extended non-ergodic states from ergodic ones. A new recursive algorithm (similar to population dynamics (PD) [21]) of treatment the Abou-Chakra-Anderson-Thouless (ACAT) equations [7] enables us to justify semi-analytically the existence of the intermediate extended non-ergodic phase for a BL with $K = 2$. Our extensive exact diagonalization numerics on the Anderson model on RRG with N up to 128 000 brought up a strong support for such a phase.

Moreover, we discovered an evidence for the *first order transition* between ergodic (EES) and non-ergodic states (NEES) within the delocalized phase. Its position corresponds to the condition for the Lyapunov exponent $L(W, E = 0) = \frac{1}{2} \ln K$ discussed in Ref.[9]. The results are summarized in Fig.1.

The model and fractal dimensions D_q–Below we analyze the properties of the eigenfunctions of the Anderson model described by the Hamiltonian:

$$\widehat{H} = \sum_{i=1}^{N} \varepsilon_i \, |i\rangle\langle i| + \sum_{i,j=1}^{N} t_{ij} \, |i\rangle\langle j|. \qquad (1)$$

Here ε_i are random on-site energies uniformly distributed in the interval $[-W/2, +W/2]$, the connectivity matrix t_{ij} equals to 1 for nearest neighbors and 0 otherwise. Each site of an infinite BL has K neighbors in the previous generation and one neighbor in the next generation. In an RRG each site is connected with $K + 1$ randomly chosen other sites. When short loops are neglected RRG becomes locally equivalent to BL.

Let $|a\rangle$ and $\langle i|a\rangle$ be the normalized eigenstates and wave function coefficients of Hamiltonian Eq.(1) in the site representation. One can introduce the moments $I_q = \sum_i |\langle i|a\rangle|^{2q}$ which generically scale with the number of the lattice sites $N \gg 1$ as $I_q \propto N^{-\tau(q)}$. For localized states $\tau(q) = 0$, while the ergodicity implies $\tau(q) = q - 1$. Multifractal non-ergodic states are characterized by the set of non-trivial fractal dimensions $0 < D_q = \tau(q)/(q-1) < 1$, e.g. $D_1 = \lim_{q\to 1} D_q$ and $D_2 = \tau(2)$. Exact diagonalization of a large RRG (see Fig.1) suggests that the fractal dimensions experience a jump from $D_q < 1$ for $W > W_E \approx 10.0$ to $D_q = 1$ for $W < W_E$ manifesting the first order *ergodic transition*.

Generalized recursive algorithm for ACAT equations–Following Ref.[7] we introduce a single-site Green function, $G_i^{(k)}(\omega) = \langle i|(\omega - \tilde{H}_k)^{-1}|i\rangle$ for a site i at a generation k of the reduced Hamiltonian, $\tilde{H}_k$ obtained from $\widehat{H}$ by disconnecting generations k and $k+1$. The random Green functions are characterized by distribution functions, $P_k(G)$. Individual $G_i^{(k)}$ obey the ACAT recursion equation [7]:

$$G_i^{(k)} = \frac{1}{\omega - \varepsilon_i - \sum_{j(i)} G_j^{(k-1)}(\omega)}, \qquad (2)$$

where $j(i)$ are sites at the generation $k-1$ connected to site i. These equations are ill-determined: the pole-like singularities in the right hand sides have to be regularized. This is usually achieved by adding an infinitesimal imaginary part to $\omega \to \omega + i\eta$. The recursion Eq.(2) might become unstable with respect to this addition. This happens for W below the critical disorder of the AL transition W_c and manifests the delocalized phase. For $W > W_c$ the solution $P(G) \propto \delta(\mathrm{Im}\, G)$ is stable. The

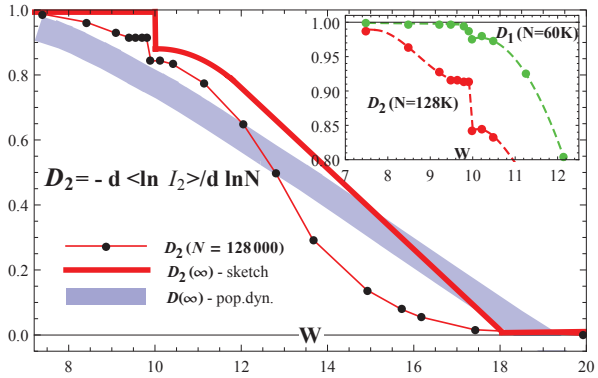

FIG. 1: (Color online) Fractal dimensions D_2 and D_1 for $K = 2$ RRG and the population dynamics exponent D as functions of disorder strength W. The W-dependence of D extrapolated to $N \to \infty$ is presented by the "brush-painted" blue line which width corresponds to the uncertainty of extrapolation. In spite of this uncertainty, D is distinctly different from 0 and 1 in a broad interval of W manifesting the non-ergodic (multifractal) nature of extended wave functions. The red solid line with black data points is a "running" fractal dimension $D_2(N, W) = -d\langle \ln I_2\rangle / d \ln N$ obtained by exact diagonalization at the maximal size $N = 128\,000$ of a disordered RRG. The fat red line is a sketch of the fractal dimension $D_2(N \to \infty, W) \equiv D_2(W)$ extrapolated to infinite N. Inset: the jump singularity in the "running" fractal dimensions $D_1(N = 60\,000, W)$ and $D_2(N = 128\,000, W)$ manifesting the ergodic transition at $W = W_E \approx 10.0$.

two types of behavior occur generically in a broad class of Anderson models [2].

The spectrum of the Hamiltonian on a finite lattice is given by a discrete set of energies, E_a corresponding to states $|a\rangle$. Although the global density of states is a sum of delta functions, $\nu(\omega) = \sum_a \delta(\omega - E_a)$, it *always* has a well-defined thermodynamic limit: one introduces an infinitesimal broadening of each delta function, η, takes first the limit of the infinite number of sites $N \to \infty$ and afterwards $\eta \to 0$. As a result, $\nu(\omega)$ tends to a smooth function. In contrast, for the local density of states (LDoS), $\nu_i(\omega) = \sum_a |\langle i|a\rangle|^2 \, \delta(\omega - E_a)$, the result of this procedure is not always a smooth function. Indeed, in the limit $W \to \infty$ the on-site states $|i\rangle$ are exact eigenstates and $\nu_i(\omega) = \delta(\omega - \varepsilon_i)$ even for the infinite system. For finite but large W, satellite δ-like peaks appear. The total number of the peaks is infinite in the thermodynamic limit but almost all of them have exponentially small weight. Hence the effective number of peaks remains finite: it increases as W is decreased and becomes infinite at $W = W_c$. At this point LDoS becomes smooth provided that the limit $N \to \infty$ is taken *before* $\eta \to 0$. Note that the opposite order of limits, ($\eta \to 0$ before $N \to \infty$) always leads to discrete peaks in LDoS.

At $W < W_c$ LDoS contains an extensive number M of peaks with significant weight: $M \to \infty$ as $N \to \infty$. Generally, one expects $M \propto N^D$ with some $0 < D \leq 1$. For

$\nu_i(\omega)$ to be smooth, the broadening η should exceed the spacing between the peaks $\delta_M \propto M^{-1} \propto N^{-D}$. Thus, the simultaneous limit $N \to \infty$, $\eta \to 0$, $N^\gamma \eta = \text{const}$ results in a smooth LDoS *iff* $\gamma < D$. Studying such generalized limits yields information on the scaling of the number of peaks, i.e. on the structure of the eigenfunctions. Wave functions of *ergodic* states are uniformly spread on a lattice, so that $M \propto N$, i.e. $D = 1$ and LDoS is smooth for any $\gamma < 1$. We show below that in a broad interval of disorder strengths in the delocalized regime $D = D(W) < 1$ and equals to the critical value of γ corresponding to the transition between a smooth and a singular LDoS, $D(W) = \gamma_c(W)$.

For $W < W_c$ (delocalized regime) and an infinitesimal $\eta > 0$, $\mathrm{Im}\, G$ increases exponentially with the number of recursion steps n in Eq.(2) describing an *infinite* tree:

$$\mathrm{Im}\, G \propto \eta\, e^{\Lambda n}. \tag{3}$$

For a *finite* RRG of size N, $n < \ln N / \ln K$ [19]. For larger n the loops terminate the exponential growth of a typical $\mathrm{Im}\, G$ limiting it by $\mathrm{Im}\, G \propto \eta\, N^{\Lambda/\ln K}$. Thus for $\nu_i(\omega) \sim N^{-D} \sum_a \eta/[(\omega - E_a)^2 + \eta^2] \approx \int dE_a\, \eta/[E_a^2 + \eta^2]$ to be smooth (and $\mathrm{Im}\, G \sim 1$ independent of η) η should scale as $\eta \propto N^{-\Lambda/\ln K}$, i.e.

$$D(W) = \Lambda(W)/\ln K. \tag{4}$$

Ideally, one would deal with infinitely small $\eta \to 0$ in order to determine the exponent Λ. However, the limited precision of any numerical computation makes it impossible in practice: for any realistic initial $\mathrm{Im}\, G \neq 0$, the value of $\mathrm{Im}\, G$ becomes significant after few recursions. To avoid this problem we included an additional step to the recursion Eq.(2):

$$\mathrm{Im}\, G_i^{(k)} \to e^{-\Lambda_k}\, \mathrm{Im}\, G_i^{(k)}, \tag{5}$$

so we keep the *typical* imaginary part fixed and k-independent: $\exp\langle \ln \mathrm{Im}\, G_i^{(k)} \rangle_k = \delta$ (where $\langle ... \rangle_k$ denotes averaging over all sites i in the k-th generation). As soon as the stationary distribution of G is reached in this recursive procedure, $\Lambda_k \to \Lambda$.

To realize this algorithm we adopted a modified *population dynamics* (PD) method [21]. In each step we used the set of N_p Green functions $G_i^{(k)}$ ("population") obtained at the previous step and new on-site energies ε_i to generate N_p new Green functions $G_i^{(k+1)}$ according to Eq.(2) in which each site is connected to K randomly chosen sites of the previous population set.

In order to obtain $D(W)$ one needs to take the limits $N_p \to \infty$, $\delta \to 0$ of $D(N_p, \delta, W)$. The convergence turns out to be slow (logarithmic) resulting in a considerable uncertainty in $D(W)$. Luckily, $D(N_p, \delta, W)$ depends only on the combined variable $X = -1/\ln(N_p^{-1} + a\delta^b)$, with $a, b \sim 1$, rather than on $\ln N_p$ and $\ln \delta$ separately. Extrapolation of $D(W, X)$ to $X = 0$ yields $D(W)$ shown in Fig.2.

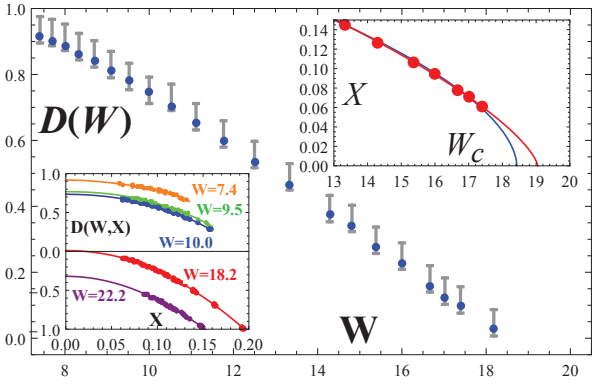

FIG. 2: (Color online) The population dynamic exponent $D(W)$ (blue points with grey error bars) extrapolated to $N = \infty$ and $\delta = 0$ for $K = 2$. The condition $D(W_c) = 0$ yields $W_c = 18.4^{+0.4}_{-0.2}$. In a broad interval of $W < W_c$ we obtained $D(W)$ distinctly different from the ergodic limit $D(W) = 1$. *Lower inset*: The collapse of data for a fixed W and different N_p, δ to a function $D(W, X)$ of $X = -1/\ln(N_p^{-1} + a\delta^b)$. Extrapolation to $X = 0$ gives the population dynamic exponent $D(W)$. The delocalized phase corresponds to $1 \geq D(W) > 0$, whereas in the localized phase $D(W) < 0$. *Upper inset*: the finite-size critical disorder $W_c(X)$ defined as $D(W_c(X), X) = 0$ and its extrapolation to $X = 0$ by the power-law fit $W_c(X) = W_c - aX^{\frac{1}{\nu}}$ with $W_c = 18.4$, $\nu = 0.56$ (blue) and $W_c = 19.0$, $\nu = 0.7$ (red). Without extrapolation the value of W_c at maximal population size $N_p^* \sim 10^8$ is $W_c(N_p^*) \approx 17.5$.

The lower inset of Fig.2 shows the collapse of the data for several N and δ from the intervals $10^3 < N < 10^8$ and $10^{-3} < \delta < 10^{-17}$. Since $b \approx 0.5$, one needs exceptionally small δ to reach small X. This required computation with higher than usual precision.

Note that the exponent Λ is a property of an infinite BL, $N = \infty$. Therefore Λ is free of the finite-size effects which dominate the moments $I_q(N)$ at $N < N_c$, where the correlation volume $N_c \sim \exp[1/\Lambda(W)]$ diverges at $W \to W_c$. The uncertainty of extrapolation of Λ to $N_p \to \infty$ and $\delta \to 0$ turns out to be small enough not to raise doubts that $0 < D < 1$ at least in the interval $10 < W < 18$ for $K = 2$. Additional support of existence of the phase with $0 < D < 1$ comes from the analytical solution to Eq.(2) in the large-K limit [23]. It turns out that in this limit:

$$D(W) = \frac{\ln\left(\frac{W_c^2}{W^2}\right)}{\ln K}. \tag{6}$$

It follows from Eq.(6) that $D(W) = 0$ and $D(W) = 1$ correspond to the values $L = \ln K$ and $L = \frac{1}{2}\ln K$ of the Lyapunov exponent $L = \ln W$ discussed in Ref.[9].

Exact diagonalization on RRG.– While ACAT approach is commonly believed to describe well the localized phase of RRG, its applicability in the delocalized regime requires further inverstigation. We performed a direct study of the Anderson model on RRG

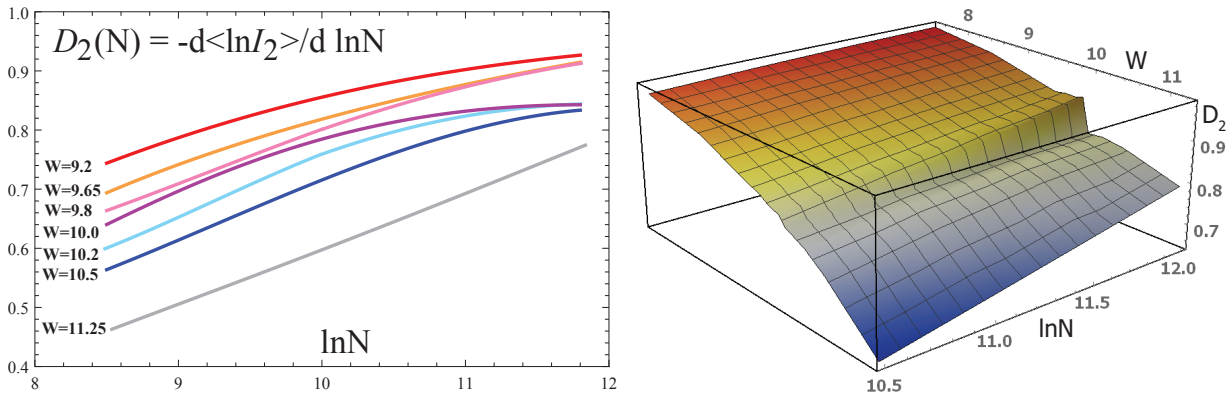

FIG. 3: (Color online) Left panel: $D_2(N,W)$ deep in the delocalized phase. The curves tend to converge to two different values of D_2 for $W = W_E + 0$ and $W_E - 0$, where $W_E \approx 10.0$. Right panel: Formation of a jump in $D_2(W)$.

by exact diagonalization at the system sizes N up to 128 000 in the range of disorder strength $7.5 < W < 20$. The main focus was on calculating the inverse participation ratio $I_2 = \sum_i |\langle i|a\rangle|^4$ and the Shannon entropy $S = -\sum_i |\langle i|a\rangle|^2 \ln(|\langle i|a\rangle|^2)$ for the eigenstates $|a\rangle$ with energies E_a near the band center. The expected asymptotic behavior of the typical averages at $N \to \infty$ is [11]:

$$\langle \ln I_2 \rangle = -D_2 \ln N + c_2, \ \langle \ln S \rangle = D_1 \ln N + c_1, \quad (7)$$

where $\langle ... \rangle$ are the averages both over the ensemble of RRG with fixed connectivity $K = 2$ and over random on-site energies ε_i, $D_{1,2}$ are the multifractal dimensions and $c_{1,2} \sim 1$. The derivatives $D_2(N,W) = -d\langle \ln I_2 \rangle / d \ln N$ and $D_1(N,W) = d\langle \ln S \rangle / d \ln N$ should saturate at D_2 and D_1, respectively in the limit $N \to \infty$.

We present the results for $D_2(N,W)$ deep in the delocalized phase (Fig.3) and close to the localization transition (Fig.4). Note two important features on these plots:

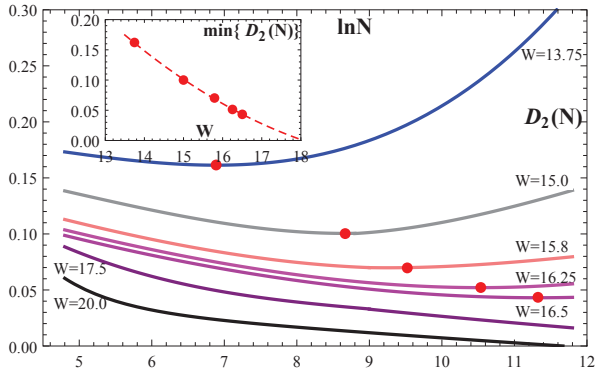

FIG. 4: (Color online) $D_2(N,W)$ close to the localization transition at $W = W_c$. The N-dependence show minima (red spot) for $W < W_c$ at $N_{\min} \to \infty$ as $W \to W_c$ [16]. Inset: $D_2(N_{\min}, W)$ as a function of W. Extrapolation by a second-order polynomial gives $W_c = 18.1 \pm 0.5$.

(i) an abrupt change of behavior for W close to 10 and (ii) a minimum in the N-dependence of $D_2(N,W)$ (recently reported in [16]) in the vicinity of AL transition: as $W \to W_c - 0$, $D_2(N_{\min}, W)$ at the minimum and $1/\ln N_{\min}$ vanish. Extrapolation of $D_2(N_{\min}, W)$ leads to $W_c = 18.1 \pm 0.5$ (see inset to Fig.4) in agreement with PD results, Fig.2.

A striking result of the exact diagonalization is the existence of a jump in both $D_2(N,W)$ and $D_1(N,W)$ shown in Fig.1. A feature, which is almost invisible at small N evolves to a more and more abrupt jump as N increases above 60 000 (see Fig. 3, right panel). Extrapolation of $D_2(N,W)$ to $N \to \infty$ for $W < 10.0$ gives $D_2 = D_2(N \to \infty, W) = 1$, whereas $D_2(W = 10.0) = 0.86 \pm 0.02$. We conclude that on RRG at $W = W_E \approx 10.0$ there is a first order transition from the non-ergodic delocalized phase at $W > W_E$ to the ergodic one at $W < W_E$.

Conclusion. The existence of the non-ergodic phase of the BL Anderson model together with the similarity of this model with generic many-body ones gives basis for far-reaching speculations. The point is that in contrast to the conventional Anderson localization, which is the property of any wave dynamics, the MBL is a genuine quantum phenomenon. Indeed, in the classical limit, a weakly perturbed integrable system with $d > 2$ degrees of freedom always demonstrates some diffusion in the phase space known as Arnold diffusion[24]. Although the celebrated Kolmogorov Arnold Moser (KAM) theorem [25] guarantees the survival of the vast majority of the invariant tori the chaotic part of the phase space is connected (unless $d = 2$), thus allowing the diffusion for arbitrary weak perturbation. Therefore one should not expect MBL in the classical limit. On the other hand the glassy states of matter without doubts exist for any $\hbar$ including $\hbar = 0$ and are obviously not ergodic. It is safe to assume that the extended non-ergodic phase of the MBL models is not qualitatively different from a classical glassy state [26]. Therefore our arguments in favor of the existence of the delocalized non-ergodic phase of the BL Anderson model and the true phase transition between

the ergodic and non-ergodic states can be considered as arguments in favor of glassy states being distinct states of matter and their transition to fluids being a true phase transition.

Acknowledgement We appreciate hospitality at KITP of University of California at Santa Barbara under the NSF grant No.NSF PHY11-25915, at KITPC in Beijing (V. E. K.) and at the Center for Theoretical Physics of Complex Systems (Daejeon, S.Korea) where the research has been carried out. E.C. thanks partial financial support by the Murcia Regional Agency of Science and Technology (project 19907/GERM/15). The research of L.B.I. was partially supported by the Russian Science Foundation grant No. 14-42-00044. We are grateful to G. Biroli, E. Bogomolny, J. T. Chalker, M. V. Feigelman, M. Foster, I. M. Khaymovich, G. Parisi, V. Ros, A. Scardicchio, M. A. Skvortsov, V. N. Smelyanskiy, K. S. Tikhonov and S. Warzel for stimulating discussions.

[1] D. M. Basko, I. L. Aleiner, and B. L. Altshuler. **321**, 1126 (2006).
[2] P. W. Anderson. Phys. Rev., **109**, 1492 (1958).
[3] V. Oganesyan and D. A. Huse. Phys. Rev. B, **75**, 155111 (2007).
[4] V. Oganesyan, A. Pal, and D. A. Huse. Phys. Rev. B **80** 115104 (2009).
[5] M. Pino, L. B. Ioffe, and B. L. Altshuler. PNAS, **113**, 536 (2016).
[6] B. L. Altshuler, Y. Gefen, A. Kamenev, and L. S. Levitov. Phys. Rev. Lett., **78** 2803 (1997).
[7] R. Abou-Chacra, D.J. Thouless, and P.W. Anderson. J. of Phys. C (Solid State Physics), **6**, 1734 (1973).
[8] M. Aizenman, S. Warzel, J. Eur. Math. Soc. **15**, 1167 (2013).
[9] M. Aizenman and S. Warzel, Europhys. Lett. **96**, 37004 (2011).
[10] G. Biroli, A. Ribeiro-Teixeira, and M. Tarzia, arXiv:1211.7334.
[11] A. De Luca, B. L. Altshuler, V. E. Kravtsov and A. Scardicchio, Phys. Rev. Lett., **113**, 046806 (2014).
[12] A. D. Mirlin and Y. V. Fyodorov, Phys. Rev. Lett. **72**, 526 (1994); A. D. Mirlin and Y. V. Fyodorov, J. Phys. I (France) **4**, 655 (1994); Y. V. Fyodorov and A. D. Mirlin, Phys. Rev. Lett. **67**, 2049 (1991); A. D. Mirlin and Y. V. Fyodorov, Phys. Rev. B **56**, 13393 (1997).
[13] E. Targuini, G. Biroli, M. Tarzia, Phys. Rev. Lett. **116**, 010601 (2016).
[14] V. E. Kravtsov, I. M. Khaymovich, E. Cuevas, M. Amini, New J. Phys. **17**, 122002 (2015).
[15] F. L. Metz, I. Perez Castillo, Large deviation function for the number of eigenvalues of sparse random graphs inside an interval. arXiv:1603.06003
[16] K. S. Tikhonov, A. D. Mirlin, and M. A. Skvortsov, Anderson localization on random regular graphs. arXiv:1604.05353 (2016).
[17] X. Deng, B.L. Altshuler, G.V. Shlyapnikov, L. Santos, Quantum Levy flights and multifractality of dipolar excitations in a random system. arXiv:1604.03820.
[18] The multifractal statistics was observed also in the numerical study [C. Monthus and T. Garel, J. Phys. A **44**, 145001 (2011)] of distribution of conductances between the root and the exturnal leeds conneceted to boundary points of a finite tree.
[19] B. Bollobas, *Random graphs*, Second edition, Cambridge studies in advanced Mathematics **73**, pp. 264-267, Cambridge University Press, 2001.
[20] M. Mezard and G. Parisi, Eur. Phys. J. B 20, 217-233 (2001).
[21] M. Mezard and A. Montanari, *Information, physics, and computation*, (Oxford University Press, 2009).
[22] see online Supplementary Material.
[23] B. L. Altshuler, L. B. Ioffe and V. E. Kravtsov (in preparation).
[24] V. I. Arnold, Instability of dynamical systems with several degrees of freedom, (Russian, English) Sov. Math., Dokl., **5**, 581 (1964); translation from Dokl. Akad. Nauk SSSR, **156**, 9 (1964).
[25] A. N. Kolmogorov. On conservation of conditionally periodic motions under small perturbations of the hamiltonian. Dokl. Akad. Nauk, SSSR, **98**, 527 (1954); V.I. Arnold, Proof of a theorem by A.N. Kolmogorov on the invariance of quasi-periodic motions under small perturbations of the Hamiltonian, Russian Math. Surveys **18**,9 (1963); J. Moser. On invariant curves of area-preserving mappings of an annulus. Nachr. Akad. Wiss., Gottingen, Math. Phys. Kl., pages 120, (1962); V. I. Arnold, *Mathematical Methods of Classical Mechanics*, Springer-Verlag (1989).
[26] M. Mezard, *First steps in glass theory*, in: M.P. Ong, R.N. Bhatt (Eds.), More is different, Princeton University Press, Princeton, New Jersey, 2001.

SUPPLEMENTARY MATERIAL

Analysis of statistics of inverse participation ratio for RRG and 3D Anderson model in the delocalized phase.

In order to evaluate the fractal dimensions $D_1(W)$ and $D_2(W)$ we performed an exact diagonalization of matrix Hamiltonians drawn from the ensemble of (i) different RRG with branching number $K = 2$ and a fixed total number of sites N ranging from 1000 to 128 000 and (ii) different realizations (~ 1000 for the largest $N = 96\,000$ and $N = 128\,000$) of the independent random on-site energies with the box distribution characterized by the disorder strength W. For the largest $N = 96\,000$ and $N = 128\,000$ we analyzed ~ 50 eigenstates with energies close to the band-center.

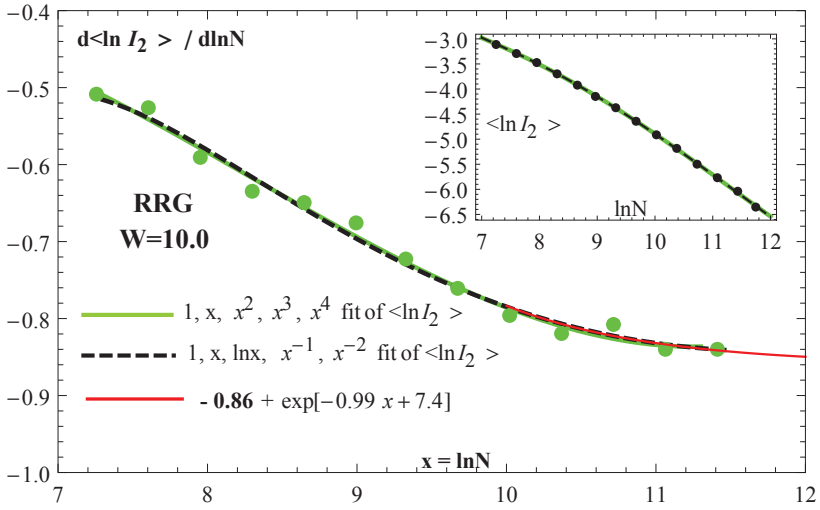

FIG. 5: (Color online) The running fractal dimension $-D_2(N,W)$ for RRG at $W = 10.0$ as a function of $x = \ln N$. Main plot: The solid green and dashed black lines are the derivatives of the two interpolating functions shown in the inset. The green spots are the discrete derivatives obtained using the raw data points. The red solid line is the best power law in N fit of the large-N tail of the (almost coinciding) green and black dashed curves. It yields $D_2 = 0.86 \pm 0.02$ distinctly different from the ergodic limit $D_2 = 1.0$. Inset: the raw data points for the ensemble averaged $\langle \ln I_2 \rangle$ and the two different interpolating functions (green and dashed black curves).

For each value of W this step of the calculation results in a set of N-dependent ensemble averages

$$\langle \ln I_2 \rangle = \left\langle \ln \sum_i |\langle a|i\rangle|^4 \right\rangle, \quad \langle \ln S \rangle = \left\langle \ln \sum_i |\langle a|i\rangle|^2 \ln(1/|\langle a|i\rangle|^2) \right\rangle, \tag{8}$$

where $\langle a|i\rangle$ are the wave function coefficients of a state a at a site i. The averages $\langle \ln I_2 \rangle$ are presented by points in the inserts of Fig.5.-Fig.7. We define the running fractal dimensions $D_2(N,W)$ and $D_1(N,W)$ as derivatives

$$D_2(N,W) = -d\langle \ln I_2 \rangle / d \ln N, \quad D_1(N,W) = d\langle \ln S \rangle / d \ln N, \tag{9}$$

respectively, since the $N \to \infty$ limits of these derivatives are by definition $D_2(W)$ and $D_1(W)$. It is convenient to first find a smooth multi-parameter approximations of the dependencies of $\langle \ln I_2 \rangle$ and $\langle \ln S \rangle$ on $\ln N$ and then evaluate the derivatives of these smooth interpolating functions. Typical 5-parameter interpolating functions are shown in Fig.5. We also evaluated discrete derivatives (green points in Fig.5-Fig.7).

The last step was to find the best power-law (exponential in $x = \ln N$) fit

$$D_{1,2}(N,W) = D_{1,2}(W) - c/N^{\gamma} = D_{1,2}(W) - \exp[-\gamma x + \text{cnst}]. \tag{10}$$

of the large-N *tail* of the smooth interpolating functions $D_{1,2}(N,W)$ (red solid curves in Fig.5.-Fig.7). Our values of fractal dimensions $D_{1,2}(W) = D_{1,2}(\infty, W)$ follow from this extrapolation. The procedure described above yields $D_{1,2}(W)$ not distinguishable form 1 for $W < 10.0$ (e.g. for $W = 9.5$ shown in Fig.6 it gives $D_2(W) = 1.0 \pm 0.02$). At the same time for $W = 10.0$ the best fit results in $D_2(10.0) = 0.86 \pm 0.02$ distinctly different from 1. We checked that the analogous procedure for the three-dimensional Anderson model in the delocalized phase with $W = 10.0$ yields $D_2 = 1.0 \pm 0.01$ (Fig.7) with all the dependencies similar to the ones for RRG at $W = 9.5$ (Fig.6). This analysis led us to the conclusion that the finite-N jump in $D_{1,2}(N,W)$ shown in Fig.1 of the main paper survives the thermodynamic limit $N \to \infty$ and implies the first order transition to the ergodic phase for $W < W_E \approx 10.0$. Another evidence of the transition at $W = W_E \approx 10.0$ is the singularity at $W = W_E$ in the speed of evolution with $\ln N$ of $D_2(N,W)$. In Fig.8 it is shown that while $D_2(N,W)$ generally increases with increasing $\ln N$, the speed of this evolution reaches a deep minimum at $W = W_E \approx 10.0$, making the convergence better at $W = 10.0$ than both for $W > 10.0$ and for $W < 10.0$. In Fig.9 we further illustrate this point: the difference $D_2(N = 128\,000, W) - D_2(N = 13\,000, W)$ shows a sharp singularity at $W = W_E$. We would like to emphasize that no extrapolation was employed.

Both features, (i) the jump in $D_{1,2}(W)$, and (ii) the anomaly in the speed of evolution, prove that the phase that exists on RRG for $W > 10.0$ may not be ergodic. We argue that the singularity of $D_2(W)$ function at $W = W_E \approx 10.0$ completely excludes the possibility of the states in the interval $W_E < W < W_c$ being ergodic.

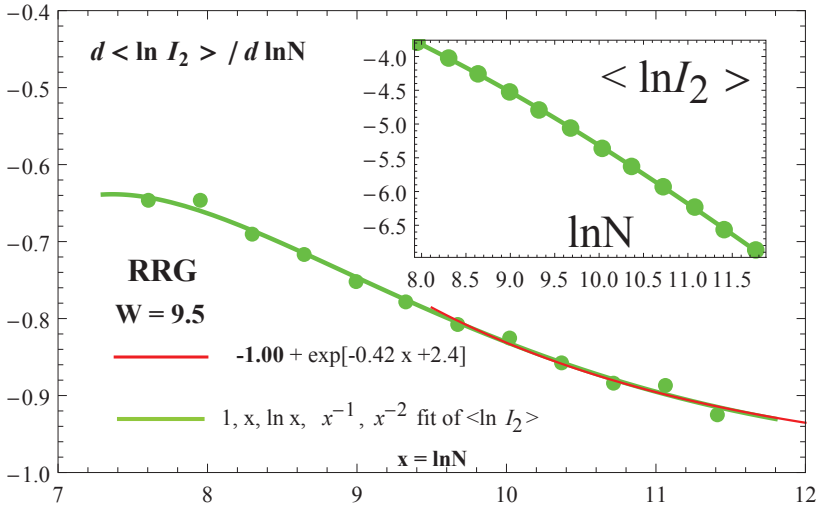

FIG. 6: (Color online)The running fractal dimension $-D_2(N,W)$ for RRG at $W = 9.5$. Main plot: the solid green line is the derivative of the smooth 5-parameter interpolating function for the ensemble averaged $\langle \ln I_2 \rangle$ shown in the inset. The red line is the best power-law in N fit of the large-N tail of the solid green line. It gives $D_2 = 1.0 \pm 0.02$.

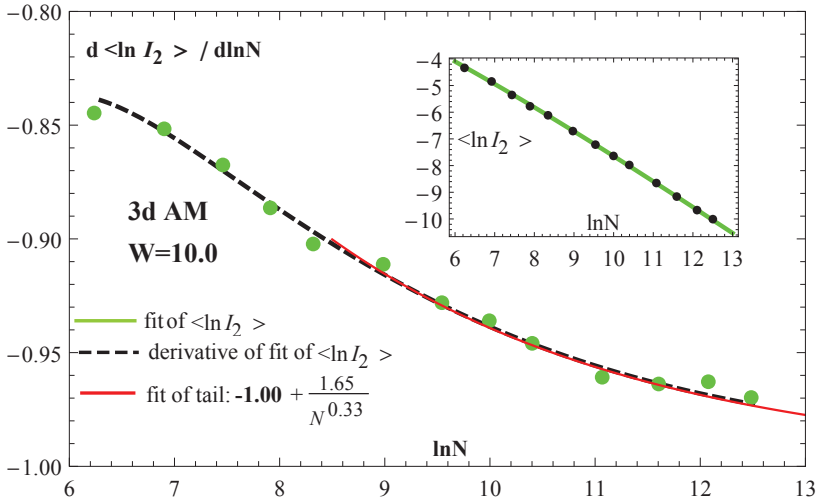

FIG. 7: (Color online) The running fractal dimension $-D_2(N,W)$ for the three-dimensional Anderson model ($W_c \approx 16.5$) in the delocalized phase at $W = 10.0$. The solid green line in the inset is the 5-parameter interpolating function for the black raw data points for the ensemble averaged $\langle \ln I_2 \rangle$. The black dashed line in the main plot is the derivative of the smooth interpolating function. The red solid line is the best power-law in N fit to the large-N tail of the black dashed line. It gives $D_2 = 1.0 \pm 0.01$ similar to the RRG with $W < 10.0$.

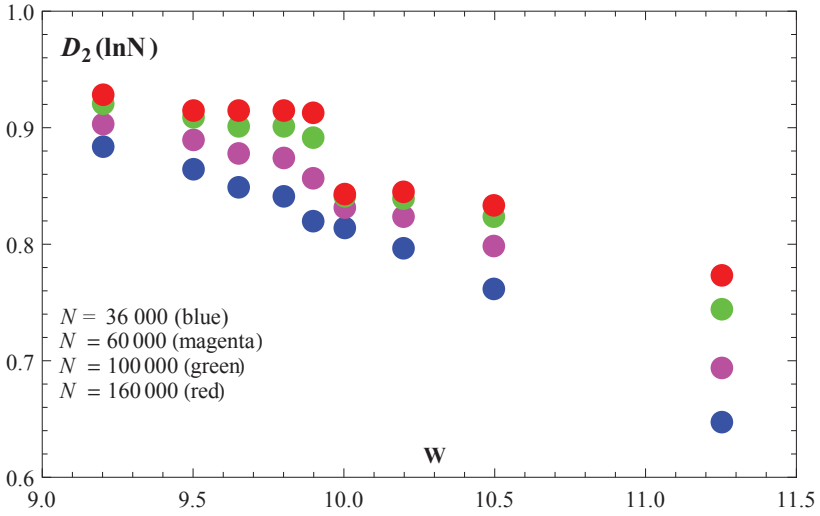

FIG. 8: (Color online) The speed of evolution of $D_2(N, W)$ with N. Blue, magenta, green and red spots correspond to $N = 36\,000, 60\,000, 100\,000, 160\,000$, respectively, in the "stroboscopic shot" of the evolution. The speed of evolution has a sharp minimum at $W = 10$.

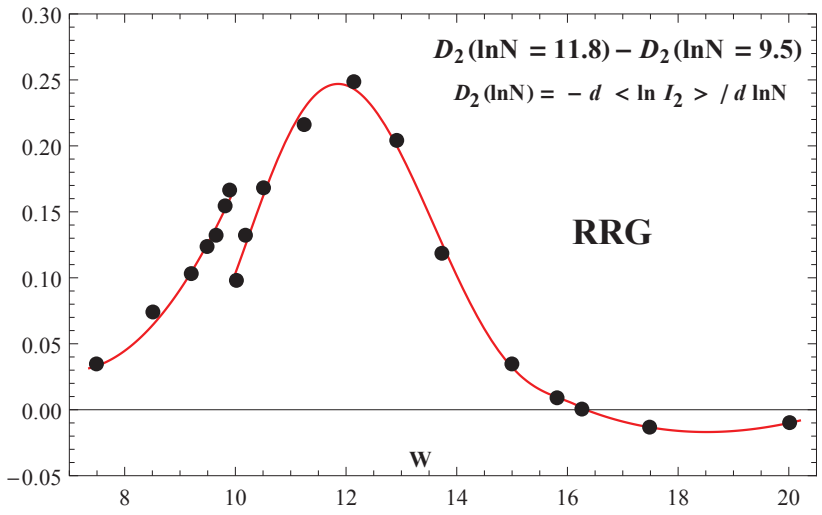

FIG. 9: (Color online) The difference $D_2(N = 128\,000, W) - D_2(N = 13\,000, W)$. It shows a sharp singularity at $W = W_E \approx 10.0$.